Putting space into modeling landscape and water quality relationships in the Han River basin, South Korea

Janardan Mainali, Heejun Chang[*]

Department of Geography, Portland State University, USA

ABSTRACT

When examining the relationship between landscape characteristics and water quality, most previous studies did not pay enough attention to the spatial aspects of landscape characteristics and water quality sampling stations. We analyzed the spatial pattern of total nitrogen (TN), total phosphorus (TP), chemical oxygen demand (COD), and suspended solids (SS) in the Han River basin of South Korea to explore the role of different distance considerations and spatial statistical approaches to explaining the variation in water quality. Five-year (2012 through 2016) seasonal averages of those water quality attributes were used in the analysis as the response variables, while explanatory variables like land cover, elevation, slope, and hydrologic soil groups were subjected to different weighting treatments based on distance and flow accumulation. Moran's Eigenvector-based spatial filters were used to consider spatial relations among water quality sampling sites and were used in regression models. Distinct spatial patterns of seasonal water quality exist, with the highest concentrations of TN, TP, COD, and SS in downstream urban areas and the lowest concentrations in upstream forest areas. TN concentrations are higher in dry winter than the wet summer season, while SS concentrations are higher in wet summer than the dry season. Spatial models substantially improved the model fit compared to aspatial models. The flow accumulation-based models performed best when the spatial filters were not used, but all models performed similarly when spatial filters were used. The distance weighting approaches were instrumental in understanding watershed level processes affecting source, mobilization, and delivery of physicochemical parameters that flow into the river water. We conclude that a consideration of the spatial aspects of sampling sites is as important as accounting for different distances and hydrological processes in modeling water quality.

1. Introduction

Various watershed level factors and in-stream processes affect the physical, chemical, and biological characteristics of water flowing in the river. Over the years, several sources, mobilization, and delivery paths and processes have been examined using different GIS-based analytical methods and spatial statistical approaches. These approaches were designed to more accurately understand, explore, and model water quality (Lintern et al., 2018a; Mainali, Chang, & Chun, 2019). Water flowing from different landscape features in the watershed carries their characteristics to the surface water bodies and affects the source, mobilization, and delivery process of different salts and nutrients to surface water bodies (Allan, 2004; Lintern et al., 2018a). Spatial distribution of the various components of the landscape, including land cover types, topography, and soil types affect the ecosystem function of the landscape and the water quality of the river basin they drain to. There are several types of metrics available, which can be extracted using a land cover map of the watershed to analyze the spatial pattern of the landscape characteristics. Most of the traditional studies use lumped values (i.e., usually percentage or the average of a specific attribute within a watershed) as a predictor of water quality.

To establish a better connection between landscape matrices and water quality, researchers have developed a distance-based and

hydrological feature-based weighting of the landscape matrices (Liberoff et al., 2019; Peterson, Sheldon, Darnell, Bunn, & Harch, 2011). The distance-weighting approaches assume that the landscape characteristics close to the stream or sampling stations exert more influence on stream quality than the regions far away. The distance weightings are generally implemented by providing higher weights to the factors (e.g., land cover type, population density) close by sampling station or rivers while providing lower weights to those that are farther away using a mathematical equation. The weighted values are then used to explore their effects on stream attributes like water quality or stream biological characteristics (Peterson et al., 2011).

Many studies use connectedness of the different landscape attributes to the sampling site or the river either using straight line distance or the distance-based on the flow length or flow accumulation. King et al. (2005) used an inverse distance weighted approach to model different water quality attributes. The distance weighted approach has been recently reinvigorated by researchers ushering to development in GIS methodology and improved understanding of the importance of hydrological processes. Peterson et al. (2011), for example, employed this approach and calculated weighted landscape metrics based on the Euclidean distance from the river and sampling station, and also weight based on the flow length and flow accumulation. Grabowski, Watson, and Chang (2016) modified some of the metrics used by Peterson et al.

---

[*] Corresponding author.
E-mail address: changh@pdx.edu (H. Chang).

(2011) by incorporating additional watershed permeability and runoff characteristics and reported that the Euclidean distance-based model worked best in modeling water temperature regime in a small watershed of Oregon USA. Watson and Chang (2018) found that the effectiveness of distance weighting of the predictor variables depends on the types of the response variable (derivatives of the stream temperature) and timescale under investigation.

Different regression modeling approaches like ordinary least squares, multiple regression, and mixed models have been used to model water quality using landscape-level explanatory variables. These methods are parametric and cannot be used when model residuals suffer from spatial autocorrelation (Anselin, 1988). A spatial regression approach should be used when a dependent variable is spatially auto-correlated, or the model residuals suffer from spatial autocorrelation (Anselin, 1988; Bini et al., 2009). Several spatial statistical methods, including spatial lag and error models, spatial eigenvector-based models, geographically weighted regression, spatial kriging, spatial autoregressive models, and spatial stream network-based models are available to model the relationship between landscape variables and water quality (Isaak et al., 2014; Mainali et al., 2019).

Our objective of this work is to model water quality parameters by exploring the role of different landscape factors and distance. We first use the eigenvector-based spatial filtering of the variables, which uses straight-line distance-based approach to constructing the eigenvector-based spatial filters to account for the spatial interrelationships in regression modeling when any of the variables suffer from spatial auto-correlation or the model itself suffers from the residual spatial auto-correlation (Getis & Griffith, 2002; Mainali & Chang, 2018). This approach has been used to model soil attributes (Kim et al., 2016), plant diversity (Kim & Shin, 2016), crime pattern (Chun, 2014), in the epidemiology (Jacob et al., 2008), and recently to model water quality trends (Mainali & Chang, 2018). Additionally, we test the distance weighted approach of landscape representations and attempt to incorporate the spatial relations of sampling sites in such models using eigenvector-based spatial filters in the water quality modeling in the Han River Basin, South Korea. We seek to answer the following research questions.

a. How are the seasonal and spatial patterns of total nitrogen, total phosphorus, chemical oxygen demand, and suspended solids concentrations in this basin?
b. What landscape variables affect different water quality parameters in the basin by season?
c. Do inclusions of the Euclidean distance-based and hydrological distance-based weighting improve model performance over lumped attributes in this basin?
d. How can 'space' be included as Eigenvector-based spatial filters in such modeling?

2. Methods

2.1. Study area

We analyze water quality data of the Han River Basin (HRB), the largest river basin in South Korea (Fig. 1). This basin was selected because it has diverse landscape characteristics, and water quality has been a big concern for people, industry, and environment (Korea Ministry of Environment, 2016; Mainali & Chang, 2018). The Han River stems from the mountainous region in the east and flows through agricultural and industrial areas in lowlands in the west. Water quality gradually degraded from upstream to downstream as the river passes through surrounding agricultural and urban areas. In particular, the water quality of some tributaries has not yet met Korean national environmental standards (Mainali & Chang, 2018). Because the main-stem Han River serves as a primary source of water for the residential and industrial areas of downstream, maintaining good water quality has

been a significant concern.

According to the land cover data of 2010, this basin is covered by 77% forest, followed by 13% agriculture, and 4% urban land cover. The HRB consists of approximately 67% poorly drained, 15% well-drained, and 18% moderately drained soil (WAMIS, 2018). It receives approximately 1200 mm of annual rainfall, with most of it falling during the summer monsoon season. The river discharge also shows a high intra-annual variability following the precipitation pattern (Bae, Jung, & Chang, 2008; Mainali & Chang, 2018).

2.2. Data sources and processing

2.2.1. Water quality data

The water quality data used in this work were obtained from the Korea Ministry of Environment Web Portal (Korea Ministry of Environment, 2016). Details of water sample collection and processing methodologies are available in Chang (2008), Korea Ministry of Environment (2016), and Mainali and Chang (2018). We analyzed 110 stations monthly for water quality parameters -total phosphorus (TP: mg/L), total nitrogen (TN: mg/L), chemical oxygen demand (COD: mg/L), and suspended solids (SS: mg/L). These parameters represent the physical, chemical, and ecological aspects of water quality. We calculated the seasonal average (fall, winter, spring, and summer) of five years of data from 2012 through 2016 for subsequent analysis. Seasonal average values were plotted in the map to explore their spatial patterns while a Kruskall-Wallis H-test was performed to test whether water quality values were significantly different in different seasons. All analyses were performed in R software version 3.6.1 (R Core Team, 2019).

2.2.2. Landscape variables

We used land cover types, elevation, slope, and soil types as the explanatory variables at the watershed level (Table 1). These variables have been most commonly used to explain water quality parameters in the literature (Mainali et al., 2019). They are significant factors influencing the source, mobilization, and delivery of different water quality components in the watershed (Allan, 2004; Lintern et al., 2018a).

2.2.3. Explanatory variables extraction and distance weighting treatments

As shown in Fig. 2, we developed four models with different distance weighting schemes (Eq. (1)). Model 1 is a traditional model that uses average values of explanatory variables within each watershed. Models 2 through 4 represent different ways of treating distance. Model 2 is based on the Euclidean distance from the sampling sites, while Model 3 is based on overland distance from the river. Model 4 uses weights based on flow accumulation. We modified a method employed by Grabowski et al. (2016) and Watson and Chang (2018) to derive watershed attributes based on different distance considerations. We provided different weighting schemes to different land-use types (urban, agriculture, and forest) and soil types in addition to elevation and slope in this work, unlike previous works that mostly used curve numbers in their analysis.

The python-based tool we used delineates the sub-watershed for each of our water quality data points using standard ArcHydro method of subwatershed delineation (Watson & Chang, 2018). This method involves creating flow accumulation and flow direction rasters using the digital elevation model (Grabowski et al., 2016). The flow lengths were then calculated using the tool of the same name available in ArcHydro toolset. Following the method by Grabowski et al. (2016) and Watson and Chang (2018), "overland flows are calculated by manipulating the input elevation dataset through the use of a mask that weights stream-defined cells as zero-distance." We created a separate raster for each land cover type by assigning a value of 1 for a specific land cover type of interest and value of 0 for other land cover types. A similar method was applied for soil types also. The elevation and soil raster data sets were, however, not modified as they have numerical
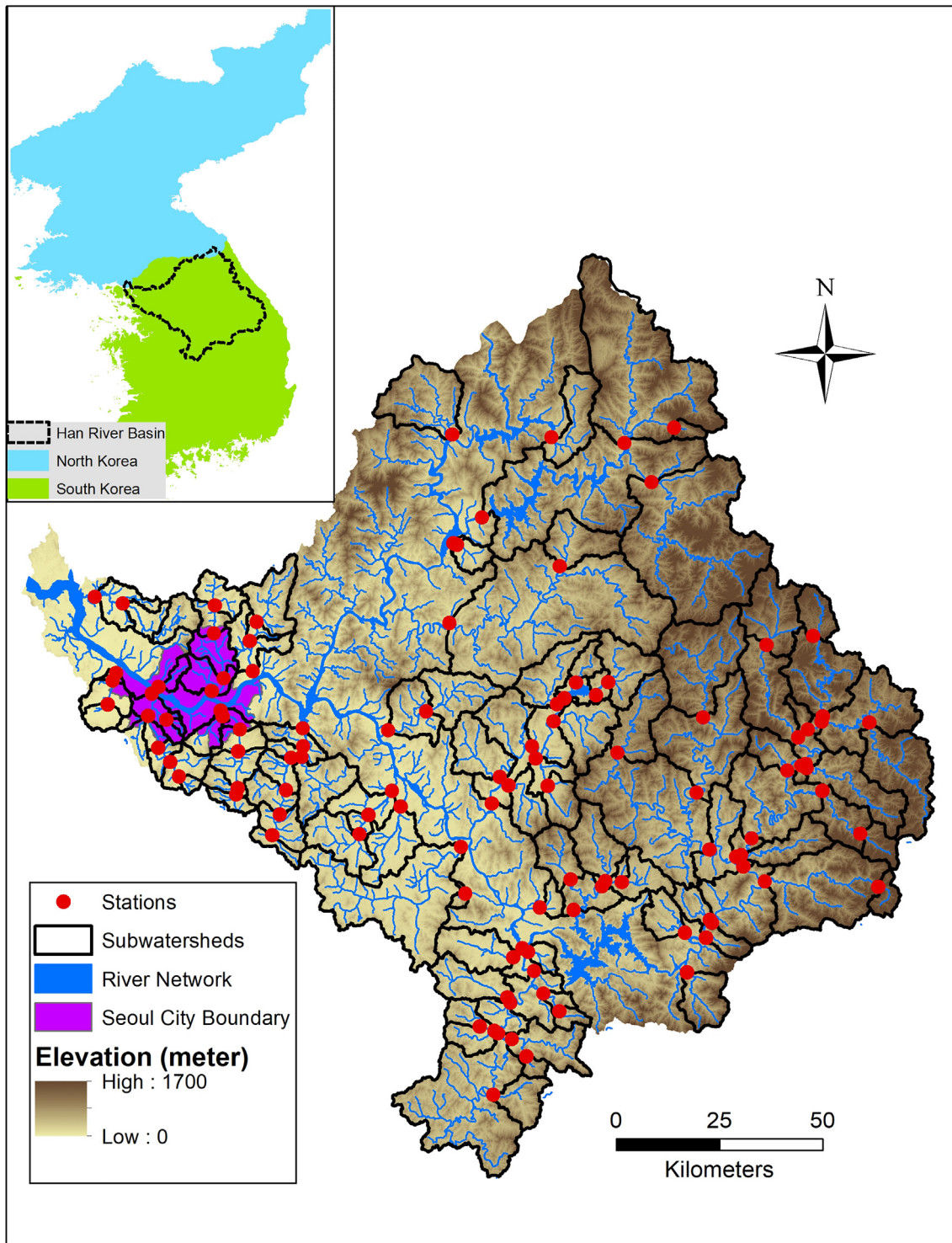
Fig. 1. Map of study area showing sampling stations.

Table 1
Different explanatory data types used in this analysis.

Data type	Source	Resolution	Unit	Descriptive statistics
Land cover	(EGIS Korea, 2017)	30 m	Percentage	Forest 77%, Agriculture 13%, Urban 4%, other 6%
Elevation	(EGIS Korea, 2017)	30 m	Meter	0 to 1700 m, 405 ± 290 m
Slope	Derived from elevation	30 m	Degree	0 to 87 degrees, 18.8 ± 11.6
Soil types	(EGIS Korea, 2017)	30 m	Percentage	Soil1 (well drained) 15%, soil2 (moderately drained) 18%, soil3 (poorly drained) 67%

Fig. 2. Graphical representation of different distance weighting treatment of watershed-level predictor variables.
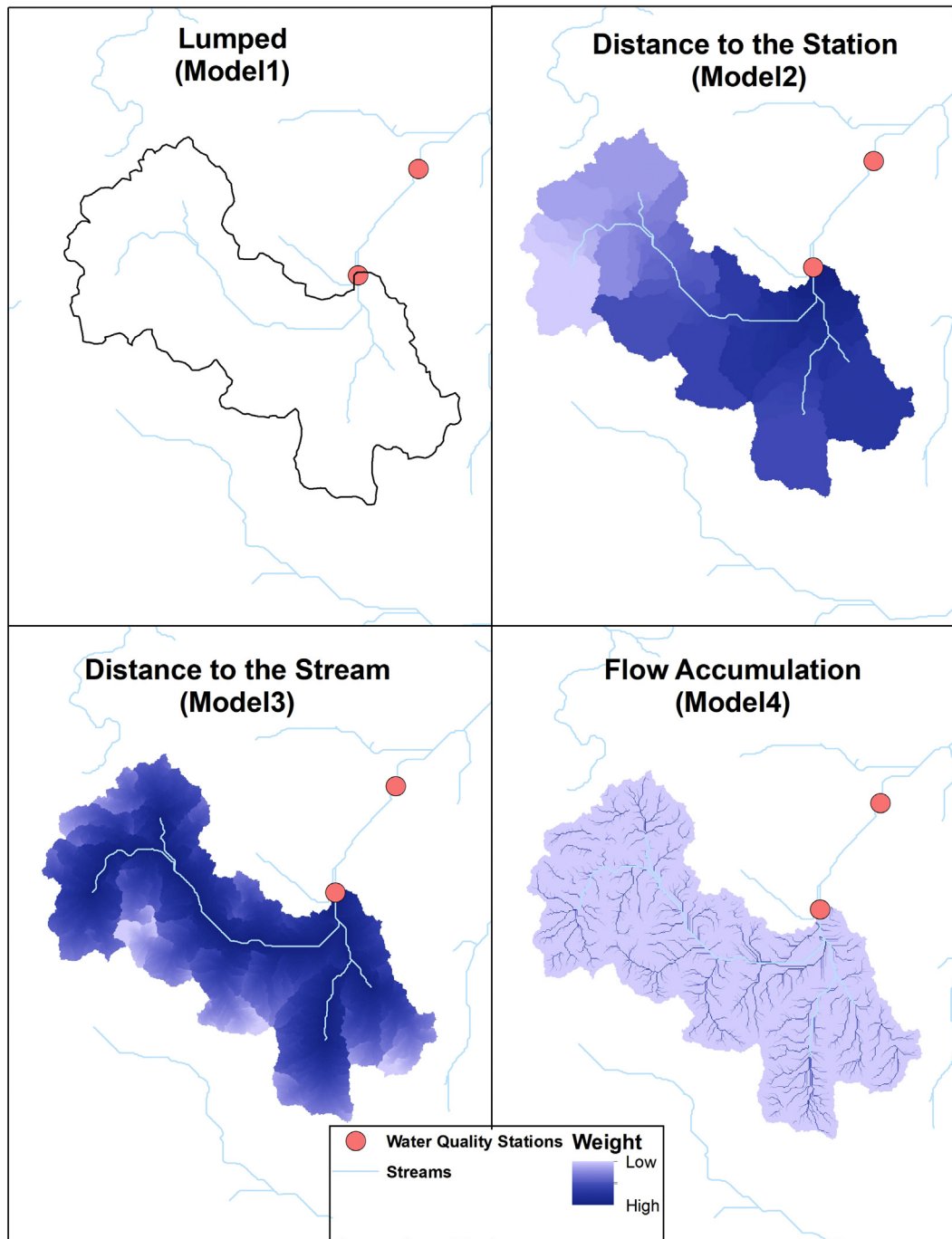
values for each raster cell. The tool finally uses an algebraic expression as in Eq. (1) to derive weight for each land cover type, elevation, slope, and soil type.

$$Weighted\ Average = \frac{\sum x_i * w_i}{\sum w_i} \tag{1}$$

For location i, x is the value of the landscape variable in question (e.g., numerical value of land cover, elevation, or slope) and w_i is the respective weight (Watson & Chang, 2018).

A total percentage of each land cover type, soil type, and an average of elevation and slope were calculated as the explanatory variables for model 1. Model 2 and 3 also used the same characteristics of land cover types, soil types, slope, and elevation but weighted them using straight line distance from the station and flow length, respectively. Model four involved weighting the same variables with the flow accumulation raster and deriving statistics for each sub-basin.

From the map of sub-basins used in this analysis, it is evident that there are some overlapping watersheds. Because overlapping watersheds are aggregated differently, they provide a different set of information. In other words, the effect of overlapping watershed fades away as distant regions have minimal weights, and regions close to sampling sites have higher weights.

2.2.4. Regression analysis

A stepwise multiple regression model was run for each seasonal water quality parameter using each model type. The response variables

were log transferred prior to the regression analysis because all of our data failed to comply with the assumption of the normal distribution as tested by the Shapiro-Wilk test. Variable inflation factor (VIF) was calculated for each explanatory variable, and variables showing high VIF (> 10) were not included in the subsequent analysis. We compare model strengths across different seasons, model types (distance weighting), and spatial considerations. Model performance matrices like model strength (R^2), Akaike Information Criteria (AIC) values, and parameter estimates of the explanatory variables were used for this comparison.

2.2.5. Spatial-filtering based regression

We tested the residual spatial autocorrelation of each regression model. As the role of landscape attributes are incorporated via distance weighting of the predictor variables, spatial patterns of the water quality sampling stations were considered as Moran's Eigenvector-based spatial filters (Getis & Griffith, 2002; Griffith, 2010). The spatial-filtering process starts with creating a weight matrix among the sampling stations based on a neighborhood criterion. In this approach, the maximum distance to select a neighborhood is determined so that every data point has at least one neighbor. This spatial configuration matrix is transformed to generate a set of n-1 eigenvectors. Because using all eigenvectors lead to model overfitting and misspecification only a set of candidate eigenvectors were selected. We used an algorithm that can reduce residual spatial autocorrelation and incorporate the spatial structure of the dependent variable under consideration (Chun, Griffith, Lee, & Sinha, 2016; Tiefelsdorf & Griffith, 2007). The Eigenvector Spatial Filtering can be expressed as in Eq. (2) (Chun et al., 2016; Mainali & Chang, 2018).

$$Y = X\beta + E_k\beta_\varepsilon + \varepsilon \qquad (2)$$

In this equation, Y is a dependent variable, X denotes a matrix of independent variables. E_k denotes the selected matrix of eigenvectors, β is a set of regression coefficients for predictor variables, β_ε is a set of regression coefficients for selected eigenvectors, and ε is random noise (error) (Chun et al., 2016). This analysis was performed using the *spatialfiltering* function of spdep package in R software (Bivand, 2017; R Core Team, 2019).

3. Results

3.1. Spatial and seasonal patterns of different water quality parameters

3.1.1. Spatial pattern

Total nitrogen (TN), total phosphorus (TP), and chemical oxygen demand (COD) concentrations are higher in the regions close to urban centers, including the Seoul metropolitan area in all seasons (Fig. 3). The suspended solids (SS) also showed similar patterns during fall, spring, and summer, while it did not show any specific spatial patterns during the summer when flow is high.

3.1.2. Seasonal pattern

The water quality parameters also showed distinct seasonal patterns when water quality parameters across all the stations were compared seasonally. TN concentration is highest during winter. The seasonal differences are significant as reported by Kruskal Wallis H-test statistics ($p < .0001$, Fig. 4). TP concentration, however, is the highest in summer, followed by the fall season. Winter and spring season concentrations are similar. The differences are statistically significant with TP as well ($p < .05$). COD concentration is the highest during the summer season. Fall and spring season COD concentrations are comparable, while winter season concentration is the lowest. The seasonal differences are significant with COD as well ($p < < 0.0001$), with a generally higher concentration in summer. SS concentration is the highest in summer, followed by spring and fall, while winter season concentration is the lowest ($p < .0001$).

3.2. Model results

3.2.1. Total nitrogen (TN)

The explanatory variables were most successful in explaining the variations in TN concentration in spring followed by winter, while fall and summer strengths were lower for aspatial models across different distance weight treatments (Fig. 5a, Table 2). Across different model types, when spatial filters were not used, model 4 (flow accumulation weighted) predicted the TN concentration higher than any other model types. However, the eigenvector-based spatial filters significantly improved model strengths across all seasons and distance weighted treatments, resulting in less noticeable differences of model strength among different model types. All the models (except for the summer of model 4) showed significant residual spatial autocorrelation, suggesting a need for a spatial regression.

Elevation and agricultural land cover are loaded as negative explanatory variables across most of the seasons and model types for TN concentration (Table 3). Soil type 2 (moderately drained) was also included positively in model 2 and model 3. However, in model 4 (flow accumulation weighted), agricultural and forest land covers were loaded as negative explanatory variables, while well-drained soil (soil1) was included as a positive variable across all seasons and spatial treatments.

3.2.2. Total phosphorus (TP)

A set of variables explained TP concentration across different seasons with R^2 values ranging from 0.4 to 0.6. When spatial filters were used, the R^2 values increased across all seasons and weight treatments. TP model strengths were highest in fall and spring for all model types related to aspatial models. But in the winter season, the aspatial model in model 2 is the highest (Fig. 5b, Table 2). The spatial filtering-based models substantially increased the model strength for all seasons, and the R^2 values are similar across different model types in spatial models. All the models showed significant residual spatial autocorrelation, prompting a need for a spatial regression to account for spatial dependencies.

As in the rest of other parameters, elevation was consistently selected as the negative variable across all seasons and spatial filtering treatments in model 1, model 2, and model 3 (Table 4). Another variable soil2 (moderately drained soil) was occasionally loaded in some seasons in model 2 and model 3. In model 4 (flow accumulation weighted), the size variable was negatively loaded for fall and spring models, forest land cover was negatively loaded for all seasons, and well-drained soil (soil1) was positively loaded for most of the seasons.

3.2.3. Chemical oxygen demand (COD)

The strength of explanatory variables to model COD concentration (R^2) is lowest for fall, while they are similarly higher in winter, spring, and summer seasons (Fig. 5c, Table 2). When aspatial models were run during the fall season, model 4 showed the highest R^2 values for aspatial models. The strengths of model 2 and model 3 were lower in aspatial models, while those of model 1 and model 4 were similar. When spatial eigenvector-based filters were used, the model strengths improved significantly higher than aspatial models for all distance weighted treatments. All the models showed significant residual spatial autocorrelation, suggesting a need for a spatial regression. In all seasons model, strengths were higher for model 1 (lumped attribute), although not significantly, than other distance weight treatments.

Elevation and size of the watershed were significant explanatory variables of COD concentration in models 1 through 3, while percentage agriculture, forest, and soil type one were identified as significant variables in flow accumulation based models (Table 5). Although none of the land cover variables significantly predicted COD concentration across models 1 through 3, a few of the variables were loaded with model 4 (Table 2). Both agricultural and forest land covers were negatively associated with COD concentration, while the presence of the
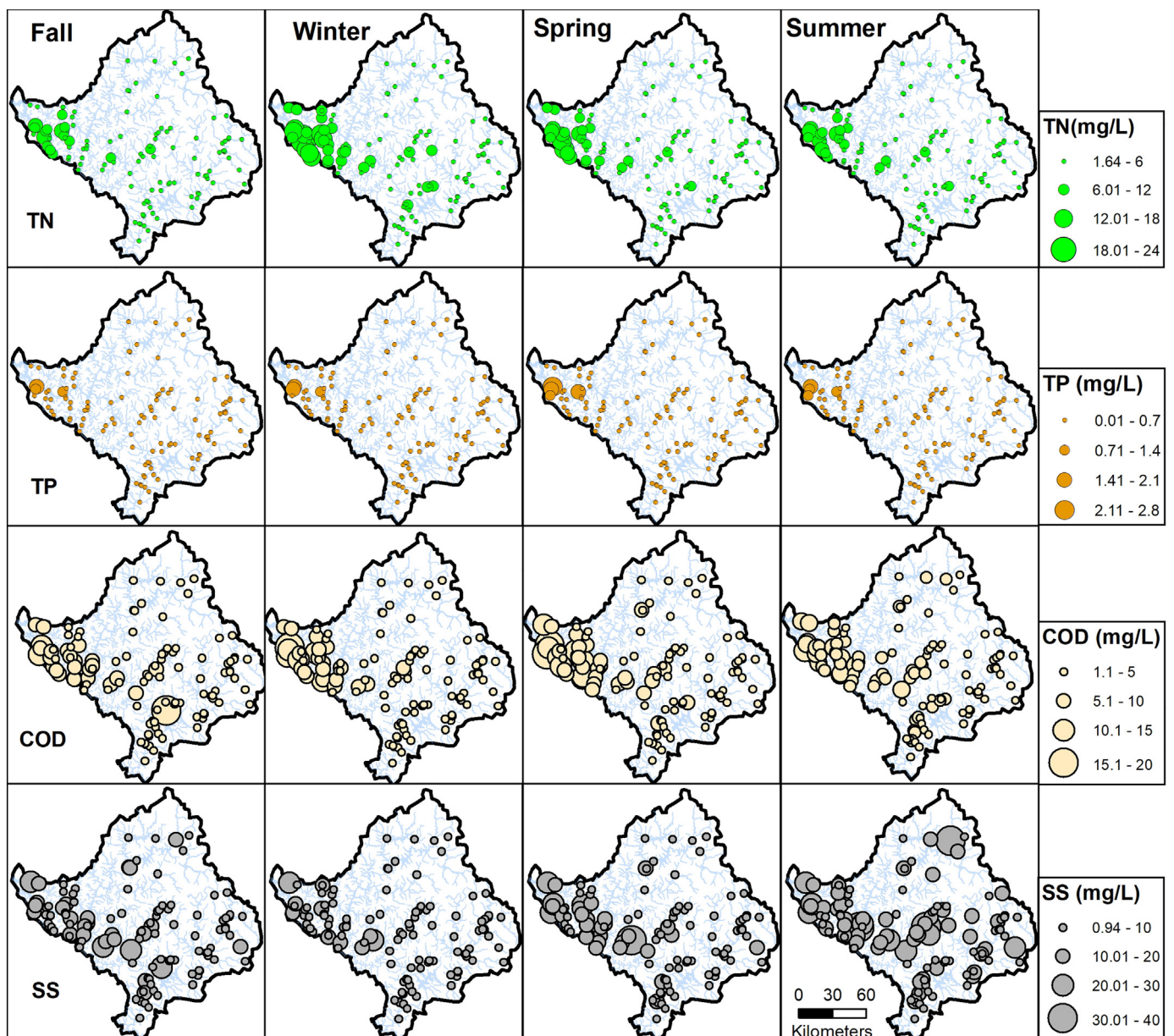
Fig. 3. Spatial patterns of different water quality parameters by season (TN: Total Nitrogen, TP, Total Phosphorus, COD: Chemical Oxygen Demand, SS: Suspended Solid).

well-drained soil at the high flow accumulation area was positively related to COD concentration.

3.2.4. Suspended solids (SS)

The explanatory variables used in this work successfully modeled SS concentration across different seasons. The model strengths were substantially higher in winter and spring, while summer season model strengths were the lowest across all distance weight and spatial filtering treatments (Fig. 5d, Table 2). The flow accumulation-based model (model 4) consistently showed the highest model strengths across different seasons when spatial filtering was not used. The spatial filtering increased model strengths substantially and leveled the effects of distance weight treatments in all seasons. All the models except for spring and summer in model 4 showed significant residual spatial autocorrelation, indicating a need for a spatial regression.

Elevation and agricultural land cover are reported as the significant predictor of SS concentrations in models 1 through 3. Model 4 (flow accumulation-based models) were loaded with the forest land cover in

all seasons and soil1 (well-drained soil) in winter in addition to agriculture land cover in fall and summer seasons (Table 6). The agricultural land cover was loaded as a positive variable for fall for model 4. As expected, flow accumulation weighted forest land cover types are significant negative explanatory variables for most of the seasons, signifying the importance of forest in ameliorating sediment loss from the landscape, especially when they are close to the stream (Hoyer & Chang, 2014).

4. Discussions

4.1. Spatial and seasonal patterns of different water quality parameters

We report higher values of different water quality parameters in the western region of the watershed around the Seoul metropolitan region, except for summer season SS. The distinct spatial patterns of different water quality parameters can be attributed to differences in land cover (Chang, 2008), topography (Mainali & Chang, 2018), restoration
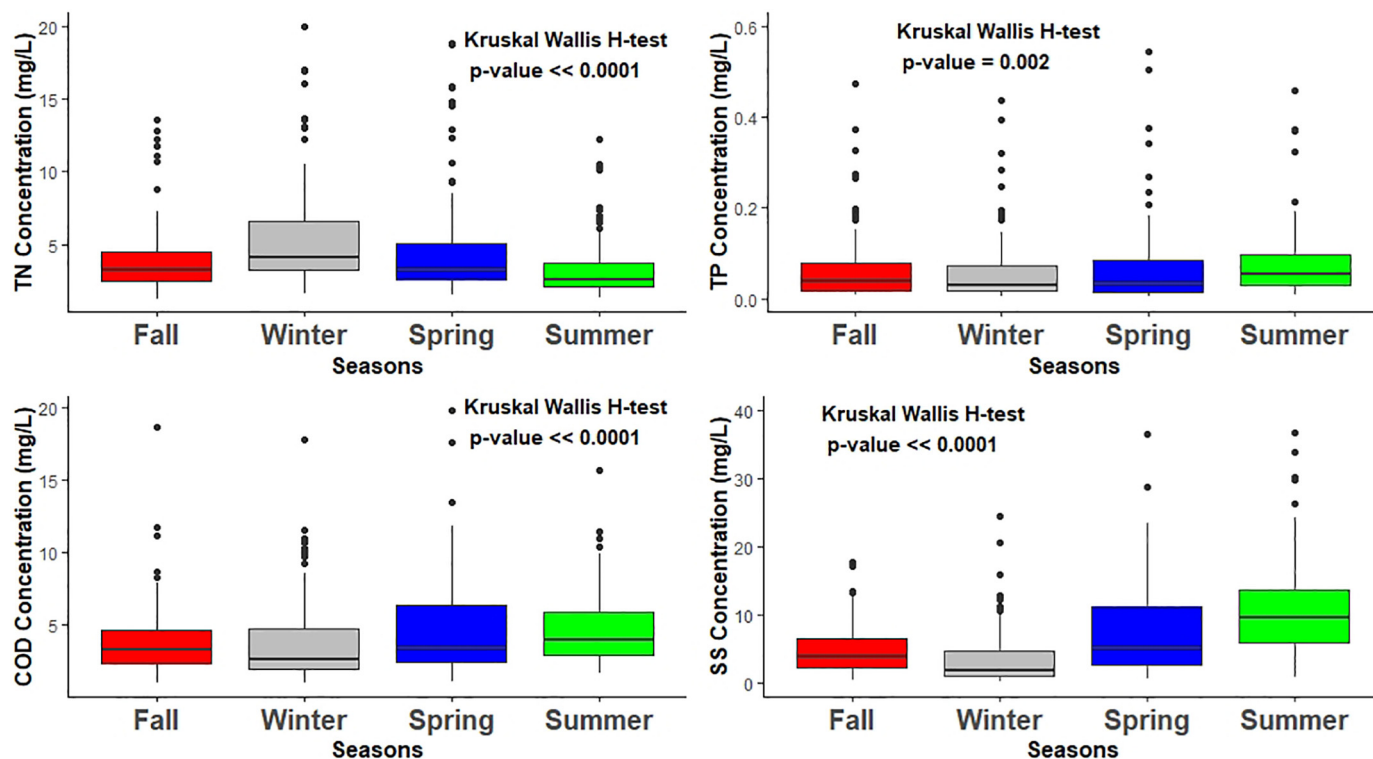
Fig. 4. Seasonal differences of different water quality parameters (TN: Total Nitrogen, TP: Total Phosphorus, COD: Chemical Oxygen Demand, SS: Suspended Solid).
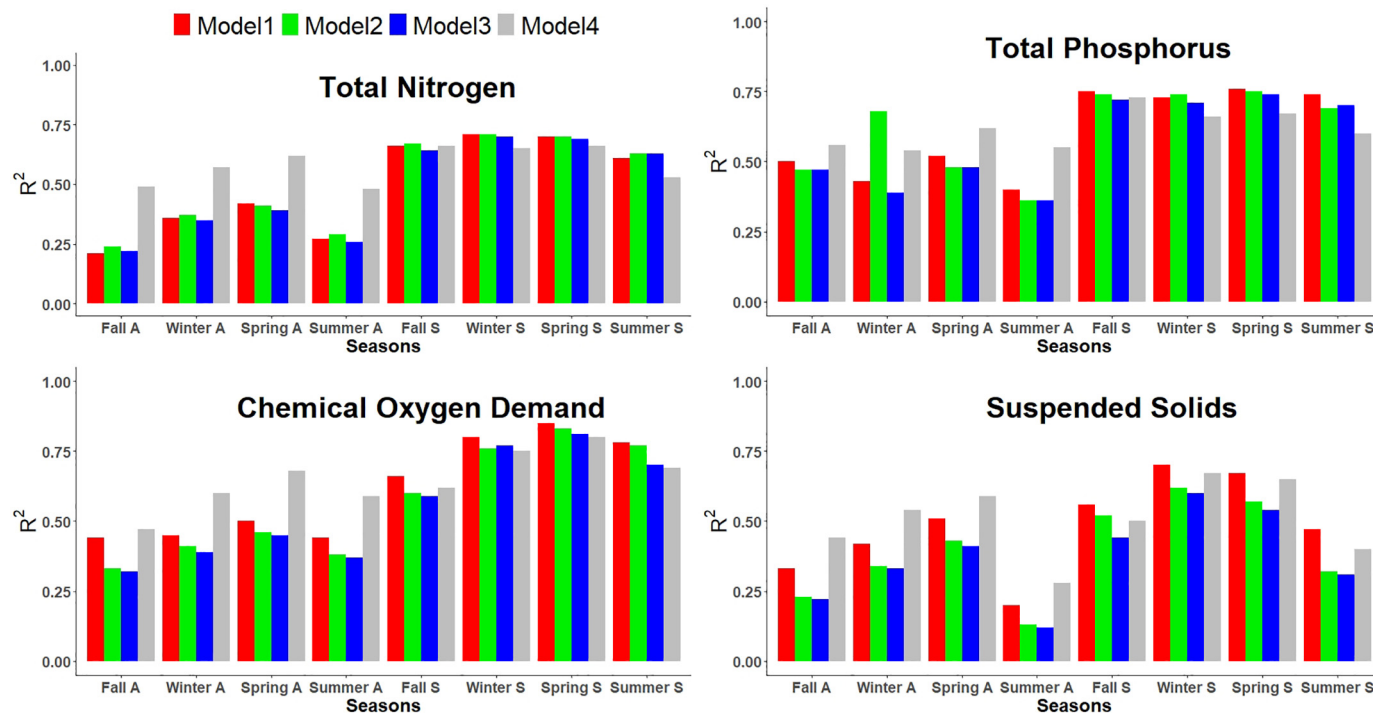
Fig. 5. R^2 values by season and spatial considerations. A: Aspatial model, S: Spatial model including spatial filters. Model 1: Aspatial Lumped Model, Model2: Inverse distance weighted model, Model3: Overland flow weighted model, Model4: Flow accumulation weighted model.

(Hong, Chang, & Chung, 2019), and policy and political regimes (Chang, Park, & Bae, 2019) in the Han River basin in South Korea. These various factors affect source, mobilization, and instream movement of different water quality parameters, leading to the varying spatial pattern in the watershed (Lintern et al., 2018a). A recent study has also reported that the number of stations exceeding the poor

category of water quality during the last five years was concentrated around the Seoul Metropolitan area (Mainali & Chang, 2018). These higher values of TN, TP, and COD in and around the major metropolitan regions can be attributed to increased urbanization (Bae & Chang, 2019). At the same time, the water quality of these urban regions have somewhat improved over time, probably due to stream restoration and

Table 2

Mean and standard deviation of R^2 values by each parameter (COD: Chemical Oxygen Demand, SS: Suspended Solid, TN: Total Nitrogen, TP: Total Phosphorus, SD: Standard Deviation).

Parameters	Values	Model1		Model2		Model3		Model4	
		Aspatial	Spatial	Aspatial	Spatial	Aspatial	Spatial	Aspatial	Spatial
COD	Mean	0.46	0.77	0.4	0.74	0.38	0.72	0.59	0.72
	SD	0.03	0.08	0.05	0.1	0.05	0.1	0.09	0.08
SS	Mean	0.37	0.6	0.28	0.51	0.27	0.47	0.46	0.56
	SD	0.13	0.11	0.13	0.13	0.13	0.13	0.14	0.13
TN	Mean	0.32	0.67	0.33	0.68	0.31	0.67	0.54	0.63
	SD	0.09	0.05	0.08	0.04	0.08	0.04	0.07	0.06
TP	Mean	0.46	0.75	0.5	0.73	0.43	0.72	0.57	0.67
	SD	0.06	0.01	0.13	0.03	0.06	0.02	0.04	0.05

Table 3

Model attributes of TN.

	Season	Sp/As	rSAC	R^2	AIC	Intercpt	$elev*10^{-3}$	$size*10^{-32}$	ag	for	soil1	soil3	Significant eigenvectors (ev)
Model1	F	A	0.41*	0.21	143	1.75	−1.04						
		S	−0.09	0.66	60	1.75	−1.04		−0.87				1.99ev2, 2.2ev4, −0.7ev16, 0.6ev10
	W	A	0.42*	0.36	141	2.15	−1.4						
		S	−0.06	0.71	63	2.15	−1.4		−0.7				2.02ev2, 1.83ev14, −0.7ev16, 0.6ev30
	Sp	A	0.36*	0.42	142	2.09	−1.5		−0.99				
		S	−0.07	0.7	78	2.09	−1.5		−0.99				1.8ev4, −0.7ev16, 0.7ev10
	Su	A	0.33*	0.27	131	1.68	−1.1		−1.17				
		S	−0.06	0.61	71	1.68	−1.1		−1.17				1.88ev4
Model2	F	A	0.4*	0.24	141	1.59	−1.2		−1.17			1.09	
		S	−0.12	0.67	56	1.63	−1.3		−0.99			1.23	2.23ev2, 2.18ev4, −0.6ev16
	W	A	0.39*	0.37	141	1.99	−1.7		1.05			1.08	
		S	−0.07	0.71	65	2.03	−1.7		−0.90			1.29	2.32ev2, 1.8ev4, −0.6ev16, 0.7ev10
	Sp	A	0.34*	0.41	143	1.95	−1.8		−1.19			0.84	
		S	−0.09	0.7	78	1.99	−1.9		−1.01			1.05	2.2ev2, 1.7ev4, 0.69ev10
	Su	A	0.32*	0.29	129	1.5	−1.3		−1.29			1.05	
		S	−0.09	0.63	67	1.55	−1.37		−1.16			1.21	1.8ev4, 0.7ev23
Model3	F	A	0.4*	0.22	143	1.53	−1.17		−0.8			0.9	
		S	−0.09	0.64	66.7	1.53	−1.19		−0.73			0.88	2.19ev2, 2.16ev4, −0.6ev16
	W	A	0.4*	0.35	144	1.94	−1.56		−0.77			0.97	
		S	−0.11	0.7	69	1.93	−1.59		−0.68			0.93	2.28ev2, 1.74ev4, −0.68ev16
	Sp	A	0.35*	0.39	148	1.87	−1.7		−0.8				
		S	−0.13	0.69	81	1.87	−1.74		−0.75			0.7	2.19ev2, 1.7ev4
	Su	A	0.32*	0.26	133	1.43	−1.2		−0.91			0.92	
		S	−0.09	0.63	66	1.43	−1.2		−0.85			0.89	1.74ev2, 1.8ev4, 0.69ev23
Model 4	F	A	0.16*	0.49	98	1.76	−0.7		−0.81	−1.6	0.84		
		S	−0.01	0.66	75	1.93			−0.76	−1.3	2.06		1.1ev2, 2.02ev4, 0.7ev10
	W	A	0.19*	0.57	100	2.1		−7.8	2.10	−1.8	0.73		
		S	−0.09	0.65	87	2.2		−9	0.69	−1.5			0.9ev2, 1.69ev4, 0.77ev10
	Sp	A	0.1*	0.62	99	1.93		−1.93	−0.83	−1.6	0.9		
		S	0.03	0.66	94	2.04		−1.12	−0.8	−1.3			0.9ev2, 1.45ev4, 0.7ev10
	Su	A	0.1*	0.48	96	1.69							
		S	−0.04	0.53	93	1.84			−0.85	−1.4	0.73		1.57ev4

* refers to $p \leq 0.05$ for residual spatial autocorrelation. The only direction of parameter estimates are provided. F- Fall, W- Winter, Sp- Spring, Su- Summer. A- Aspatial model, S- Spatial model. elev- elevation, ag- agriculture land use, for- Forest. soil1- well-drained, soil 3- poorly drained.

implementation of strict water quality guidelines by the government (Mainali & Chang, 2018). Recent research demonstrates increased interest in local stream environments by stakeholders, and various stream restoration projects are underway, especially in more developed regions in the Seoul metropolitan area (Hong et al., 2019).

4.2. Water quality models

Our result shows that forest land cover types are negatively associated with TN concentration when they are treated with flow accumulation-based weighting schemes. As expected, forest land cover, when located close to streams, significantly reduces the nutrient flow to streams (Kuglerová, Ågren, Jansson, & Laudon, 2014). Agricultural and urban land covers are typically associated with the high nitrogen concentration in streams (Galloway et al., 2003; Mainali & Chang, 2018; Xu, Yin, Ai, Xin, & Shi, 2016). However, low nitrogen flow from agricultural lands to the river during some seasons may be associated with the following three factors. First, water is held in agricultural land during the rice sowing period. Second, nitrogen may be unavailable in the agricultural areas land due to a lack of application of nitrogen-based fertilizers or manure. Third, there may have been meager rainfall to wash nitrogen from croplands.

Our result suggests that the presence of forest land cover in the high flow accumulation area (vicinity of the stream) significantly reduces TP concentration. But, it also shows that those areas need to have well-drained soil. An increase in phosphorus with fine-grain soil has been reported in Finland (Röman, Ekholm, Tattari, Koskiaho, & Kotamäki, 2018). Previous studies identified the importance of forest in ameliorating phosphorus loads in stream water, while agricultural land cover is the primary source of phosphorus to the water (Ockenden et al., 2017; Powers et al., 2016).

Although none of the land cover variables significantly explained the variation of COD concentration across models 1 through 3, a few explanatory variables were included with model 4, signifying the

Table 4
Model attributes of TP.

	Season	Sp/Asp	rSAC	R^2	AIC	Intercept	elev*10^{-3}	size*10^{-32}	ag	for	soil1	soil2	soil3	Significant eigenvectors (ev)
Model1	F	A	0.32*	0.50	197	−2.19	−2.5							
		S	−0.08	0.75	264	−2.19	−2.8							2.9ev2, 2.8ev4
	W	A	0.38*	0.43	3.4	−2.29	−2.9							
		S	−0.07	0.73	228	−2.28	−2.9							4.2ev2, 4.07ev4, −1.8ev16
	Sp	A	0.35*	0.52	283	−1.95	−3.7							
		S	−0.09	0.76	213	−1.94	−3.1							3.5ev2, 3.16ev4
	Su	A	0.34*	0.40	259	−2.14	−2.3							
		S	−0.12	0.74	180	−2.14	−2.6							2.6ev2, −1.3ev14, −1.3ev16
Model2	F	A	0.33*	0.47	272	−2.38	−3.2							
		S	−0.07	0.74	202	−2.37	−3.4					1.35		3.6ev2, 2.7ev4, −1.54ev16
	W	A	0.28*	0.68	310	−1.75	−3.6							
		S	−0.1	0.74	224	−2.54	−3.7					1.9		5.05ev2, 3.83ev4, −1.9ev16
	Sp	A	0.36*	0.48	291	−2.19	−3.7							
		S	−0.06	0.75	218	−2.19	−3.8					1.43		4.3ev2, 2.9ev4
	Su	A	0.32*	0.36	269	−2.22	−2.7							
		S	−0.11	0.69	200	−2.22	−2.8							3.13ev2, 2.6ev4, −1.4ev16
Model3	F	A	0.33*	0.47	273	−2.49	−3.15							
		S	−0.09	0.72	209	−2.49	−3.23					1.12		3.6ev2, 2.5ev4, −1.8ev16
	W	A	0.4*	0.39	312	−2.65	−3.4							
		S	−0.08	0.71	237	−2.65	−3.5					1.6		4.9ev2, 3.73ev4, −1.9ev16
	Sp	A	0.35*	0.48	294	−2.31	−3.6							
		S	−0.09	0.74	226	−2.3	−3.67							4.2ev2, 2.9ev4
	Su	A	0.33*	0.36	268	−2.29	−2.67							
		S	−0.12	0.70	197	−2.29	−2.7							3.1ev2, −1.3ev14, −1.48ev16
Model4	F	A	0.08*	0.56	254	−2.3		−1.9		−2.5	1.59			
		S	0.003	0.73	241	−2.54		−2.2		−2.3	1.12			2.3ev4, −1.4ev16, −2.5ev1
	W	A	0.27*	0.54	282	−2.24				−3.4	1.9			
		S	0.08	0.66	259	−2.4				−3.03				2.3ev2, 3.6ev4, −1.4ev16, −2.2ev1
	Sp	A	0.21*	0.62	260	−2.5		−2.4	−0.37	−2.71				
		S	0.09	0.67	252	−2.72		−2.7		−2.5	1.87		1.2	2.4ev4, −1.99ev1
	Su	A	0.2	0.55	230	−2.45				−2.54	2.12			
		S	0.09	0.6	227	−2.6				−2.45	1.74		0.85	−1.25ev14, 1.94ev4, −1.56ev1

* refers to p ≤0.05 for residual spatial autocorrelation. F- Fall, W- Winter, Sp- Spring, Su- Summer. A- Aspatial model, S- Spatial model. elev- Elevation, ag- Agriculture land use, blt- Built up area land use, for- Forest. soil1- well drained, soil2- moderately drained, soil 3- poorly drained.

importance of land cover, especially in relation to the hydrological processes (Table 2). Both agricultural and forest land covers negatively affect COD concentration, while the presence of the well-drained soil at the high flow accumulation area positively affects COD concentration. In this watershed and others in the region, COD concentration is usually related to urban areas (Chang, 2008; Chen & Lu, 2014; Liu et al., 2017), which is manifested in our result as negative loading of flow accumulated forest and agriculture land cover in the absence of significant urban land cover. High flow accumulation is usually along the stream in riparian areas. The forest cover in those areas always helps by ameliorating the flow of nutrient loading to the surface water bodies consistent with our result (Brogna et al., 2017; de Mello, Valente, Randhir, dos Santos, & Vettorazzi, 2018).

The agricultural land cover was loaded as a positive explanatory variable for fall for most of the model types and seasons, suggesting the role of agricultural practices in increasing suspended solid concentration in the river. The importance of forest in ameliorating sediment loss from the landscape, especially when they are close by the stream, has been seen in this result as well because flow accumulation weighted models suggested forest land cover as significant negative predictors. Chang (2008) also reported a lower SS concentration in the forested catchment at the watershed as well as a riparian buffer scale in the study basin.

4.3. Distance weighting and spatial consideration

Consistent improvements in model performance as we include flow accumulation-based distance weighting treatments might be attributed to the fact that the major process of mobilization and delivery of these parameters are captured in the model. Past research consistently showed that the distance weighting treatment generally improves the model performance of water quality parameters (Grabowski et al.,

2016; King et al., 2005; Peterson et al., 2011). However, the most effective distance weighting treatments differ by the types of parameters being modeled and/or season at which water attributes from a stream are collected. For example, fish indicators and physicochemical parameters were better modeled with the inverse distance weighted and hydrologically active inverse-distance metrics than with the simple Euclidean distance weighted matrices. However, the opposite was the case for invertebrate assemblages (Peterson et al., 2011). Grabowski et al. (2016) also concluded that the spatially explicit landscape indicators (aka distance weight treatments) that also account for watershed processes improved the predicting power of the regression models. Watson and Chang (2018), however, reported mixed results of the weighting schemes, with model results varying along with the water quality parameters and seasons.

Most of the nutrients and salts are delivered to rivers via an overland flow in a drainage basin. The overland flow accumulates towards the proximity of the river. The current study shows that when we provide higher weight towards different parameters based on flow accumulation, they can explain water quality parameters better than other weight treatments. We also need to pay attention to which explanatory variable weights produced the most robust models. In this work, we notice that these variables are different for different parameters, and they differ by seasons as well. This finding is congruent with the general understanding of the effects of these factors on river water quality in this watershed and other parts of the world (Chang, 2008; Lintern et al., 2018b; Mainali & Chang, 2018; Pratt & Chang, 2012).

Most of the models showed significant residual spatial autocorrelation in our analysis. When Grabowski et al. (2016) tested for the same, they did not report any significant spatial autocorrelation. Recent studies have reported that the residual spatial autocorrelation can be due to spatial autocorrelation of dependent variables, the scale of

Table 5
Model attributes of COD.

Model	Season	Sp/Asp	rSAC	R²	AIC	Intercept	elev*10⁻³	size*10⁻⁵	ag	blt	for	soil1	Significant eigenvectors
Model1	F	A	0.29*	0.44	136.34	1.68	−1	9.3					
		S	−0.11	0.66	79.2	1.68	−1	9.3					2.03ev2, 1.13ev8, 0.96ev4, 0.83ev13, 0.74ev10, 0.75ev10, 0.97ev30
	W	A	0.4*	0.45	165.1	1.8	−2	9.5					
		S	−0.11	0.8	71	1.8	−2	9.5					2.7ev2, 1.32ev4, 1.1ev8, −1.02ev16, 1.0ev20, −0.7ev9, 0.79ev14, 1.02ev30, −0.76ev21
	Sp	A	0.45*	0.5	144	1.95	−2	9.5					
		S	−0.14	0.85	25.6	1.96	−2	9.5					2.7ev2, 1.3ev4, .9ev8, −.84ev16, .7ev14, .77ev13,-.61ev5, .64ev10, .6ev1, −.72ev21, −.54ev9, 0.8ev30, 0.57ev20, −.55ev25, .71ev36, .75ev39, −.56ev35
	Su	A	0.34*	0.44	97	1.81	−2						
		S	−0.14	0.78	12.3	1.81	−2	5.7					1.7ev2, .98ev4, 0.98ev14, 0.7ev10, 0.6ev8, −.54ev5, 0.5ev13, −0.5ev16, 0.7ev34, 0.5ev36, −0.5ev35, 0.6ev39
Model2	F	A	0.27*	0.33	144	1.7	−2						
		S	−0.1	0.6	94	1.7	−2	7.7					1.74ev3, 1.5ev2,-1.3ev8, 1.06ev13, −0.7ev23
	W	A	0.37*	0.41	172	1.78	−2						
		S	−0.1	0.76	81.3	1.78	−2	7.2					2.3ev3, 2.08ev2, −1.3ev8, 1.3ev13, 0.9ev18, −0.98ev18, 0.73ev6,-0.87 ev23, 0.9ev34, −0.97ev38
	Sp	A	0.42*	0.46	155	1.98	−2						
		S	−0.21	0.83	45	1.98	−2	7.6					2.25ev3, 2.02ev2, −1.08ev8, 1.09ev13, 0.72ev6, −0.57ev1, 0.7ev18, −0.55ev4, 0.76ev23, 0.55ev21, 0.9ev38, −0.65ev34, −0.65ev36, −0.75ev39
	Su	A	0.32*	0.38	107	1.83	−1.3						
		S	−0.11	0.77	31.5	1.83	−1.3						1.63ev3, 1.3ev2, 1.1ev13, −.76ev8, 0.65ev10, 0.55ev6, −.57ev23, −.8ev39, 0.7ev38
Model3	F	A	0.28*	0.32	146	1.63	−1.3						
		S	−0.07	0.59	95	1.63	−1.3						−2.28ev2, 1.3ev8, 1.07ev13,-0.86ev6, −0.78ev3
	W	A	0.39*	0.39	175	1.7	−2						
		S	−0.1	0.77	81	1.7	−						−3.07ev2, 1.3ev8, 1.2ev13, −0.9ev3, −0.9ev6, −0.8ev18,0.9ev34, 1.1ev38
	Sp	A	0.42*	0.45	157	1.91	−2						
		S	−0.1	0.81	50.6	1.91	−2	7.2					−2.9ev2, −1.06ev6, 1.09ev8, −0.9ev3, 1.09ev13, −0.57ev18, −.65ev23, 1.18ev38, −0.65ev35
	Su	A	0.31*	0.37	33.18	1.8	−1						
		S	−0.08	0.7	109	1.8	−1.3						−1.96ev2, 1.16ev13. -0.82ev6, −0.7ev3, 0.8ev8, −0.6ev10, −0.6ev23, 1.01ev38
Model4	F	A	0.15*	0.47	121.4	1.86			−0.54		−1.28		
		S	−0.1	0.62	89	1.86			−0.54		−1.28		−1.23ev1, −1.2ev11, −0.8ev5, −0.8ev6, −0.77ev7, −0.68ev22
	W	A	0.21*	0.6	131	1.56			−0.7		−1.65		
		S	−0.09	0.75	85	1.56			−0.7		−1.65	0.99	−1.26ev1, −1.5ev11, −1.19ev5, −8.12ev6,0.7ev3, −0.8ev15
	Sp	A	0.19*	0.68	98.05	1.69					−1.68	1.22	
		S	−0.11	0.8	56.7	1.62			−0.31		−1.68	1.22	−1.3ev11, −0.9ev1, −0.9ev5, −0.8ev6, 0.57ev3-0.5ev7,
	Su	A	0.11*	0.59	65	1.81					−1.1	−0.75	
		S	−0.08	0.69	37	1.81					−1.2	−0.75	−1.1ev11, −0.72ev5, −0.6ev1, −0.54ev8

* refers to p ≦0.05 for residual spatial autocorrelation. The only direction of parameter estimates is provided. F- Fall, W- Winter, Sp-Spring, Su- Summer. A- Aspatial model, S- Spatial model. elev- Elevation, ag- Agriculture land use, blt- Built up area land use, for- Forest. soil1- well-drained soil.

Table 6
Model attributes of SS.

Model	Season	Sp/Asp	rSAC	R^2	AIC	Intercept	elev*10^{-3}	size*10^{-8}	ag	for	soil1	Significant eigenvectors
Model1	F	A	0.16*	0.33	221	1.22	−9		3.33			
		S	−0.08	0.56	184	1.22	−9		3.33			1.95ev2, −1.97ev14, 1.23ev4, 1.22ev19, −1.02ev16, 1.47ev30
	W	A	0.33*	0.42	253	1.11	−1.8		3.09			
		S	−0.13	0.7	192	1.11	−1.8		3.09			3.66ev2, −1.17ev14, 2.2ev4, −1.4ev16
	Sp	A	0.16*	0.51	205	2.01	−1.9		2.4			
		S	−0.09	0.67	170	2.01	−1.9		2.4			2.1ev2, −1.51ev14, 1.22ev19, 1.17ev1
	Su	A	0.15*	0.2	210	1.88		1.6	2.9			
		S	−0.07	0.47	171	1.88	−3.9	1.6	2.9			0.47ev2, −2.4ev14, 0.9ev4, 1.24ev19, 1.29ev30, 1.55ev1
Model2	F	A	0.14*	0.23	237	1.39	−1.3		1.63			
		S	−0.12	0.52	199	1.39	−1.4	1.3	1.73			2.7ev2, −1.79ev14, 1.12ev19, −1.2ev16, 1.7ev30, −1.19ev17
	W	A	0.29*	0.34	268	1.27	−2.3					
		S	−0.09	0.62	214	1.27	−2.4		1.45			4.3ev2, −1.98ev4, −1.5ev16
	Sp	A	0.13*	0.43	223	2.17	−2.4					
		S	−0.1	0.57	201	2.17	−2.4		0.97			−1.41ev14, 1.15ev19
	Su	A	0.11*	0.13	220	1.99	−7.4	1.8	1.4			
		S	−0.08	0.32	200	1.99	−7.5	1.8	1.4			−2.3ev14, 1.17ev19, −1.44ev16, 1.4ev30, 1.5ev1
Model3	F	A	0.14*	0.22	238	1.43	−1.3		1.59			
		S	−0.09	0.44	211	1.43	−1.3		1.73			2.3ev2, −1.9ev14, −1.2ev16, 1.7ev30,-1.13ev17
	W	A	0.28*	0.33	270	1.28	−2.2		1.4			
		S	−0.08	0.6	220	1.28	−2.3		1.6			4.14ev2, −2.0ev14, −1.6ev16
	Sp	A	0.12*	0.41	227	2.2	−2.3					
		S	−0.07	0.54	205	2.2	−2.3					2.5ev2, −1.5ev14, 1.3ev9
	Su	A	0.1	0.12	222	2.07	−7.2	1.7	1.31			
		S	−0.08	0.31	202	2.07	−6.9	1.6	1.33			−2.3ev14, 1.2ev19, 1.47ev30, 1.43ev1
Model4	F	A	0.02	0.44	205	2.1	−4.4		0.7	−2.32		
		S	−0.06	0.5	196	2.1	−4.4		0.8	−1.8		−1.6ev14, −1.34ev23
	W	A	0.17*	0.54	232	0.77				−3.17	1.8	
		S	−0.08	0.67	199	0.7				−2.7	1.71	1.95ev2, 1.9ev4, −1.4ev16,
	Sp	A	0.007	0.59	190	2.68				−2.22		
		S	−0.064	0.65	175	2.68				−1.8		−1.22ev14
	Su	A	0.05	0.28	204	2.3			0.9	−1.49		
		S	−0.08	0.4	187	2.3			0.7	−1.37		−2.13vc14, −1.09ev23

* refers to p ≤ 0.05 for residual spatial autocorrelation. The only direction of parameter estimates are provided. F- Fall, W- Winter, Sp- Spring, Su- Summer. A-Aspatial model, S- Spatial model. elev- Elevation, ag- Agriculture land use, blt- Built up area land use, for- Forest. soil1- well drained, soil2- moderately drained, soil 3- poorly drained.

analysis, inability to account for predictor variables with spatial structure, or inappropriate sampling design due to a model mis-specification (Bini et al., 2009; Mainali & Chang, 2018; Miralha & Kim, 2018; Thayn & Simanis, 2013). While analyzing the same set of data for the 'spatial autocorrelation of the temporal trends,' Mainali and Chang (2018) reported the significant autocorrelation in most of the temporal trends. Most of their models (they did not use any distance weight treatment) also suffered from residual spatial autocorrelation. We posit that the residual spatial autocorrelation reported in this analysis is due to the inherent properties of the data set as there is significant spatial clustering of seasonal water quality parameters associated with the agriculture or urban land use (Chang, 2008; Mainali & Chang, 2018).

Our results show that the distance-weighted treatments did not have any significant association with the model strength when spatial filters were used. However, most of the variables were loaded in the flow accumulation-based model (model 4) even without the spatial filters and hence helped explain the effect of various landscape matrices on water quality. These matrices, along with the process of flow accumulation (as in model 4), collectively explain the source, mobilization, and delivery process of different water quality parameters. This is not possible in other models where different explanatory variables suffer from multicollinearity, and only a couple could be loaded in each model.

5. Conclusions

We found significant spatial patterns of different water quality parameters with a high concentration of chemical oxygen demand, suspended solids, total nitrogen, and total phosphorus in the southwest area of the basin around the Seoul metropolitan area and other urban centers. Water quality parameters also showed seasonal patterns with

the highest concentration in winter, spring, or summer season depending on the parameters. Collectively, land cover, soil, and topographical variables could explain the variation of these parameters, successfully explaining 50 to 80% of variations in water quality. The strengths of these models were highest when flow accumulation-based weightings were used for the predictor variables. When spatial filters were used in conjunction with the distance weighting, all distance weighting-based models showed similar model strengths, which were generally higher than only distance weighting treatments. We conclude that the distance weighted treatments and eigenvector-based spatial filtering approaches could be used complimentarily to understand the spatial patterns of water quality parameters as well as to explore watershed level processes affecting them. Although we do not anticipate these relations to be universal, we recommend considering 'space' with spatial statistical methods while modeling water quality using (weighted) landscape matrices.

References

Allan, J. D. (2004). Landscapes and riverscapes: The influence of land use on stream ecosystems. *Annual Review of Ecology, Evolution, and Systematics, 35*(1), 257–284. https://doi.org/10.1146/annurev.ecolsys.35.120202.110122.
Anselin, L. (1988). *Spatial econometrics: Methods and models.* Dordrecht: Kluwer Academic.
Bae, D.-H., Jung, I.-W., & Chang, H. (2008). Long-term trend of precipitation and runoff in

Korean river basins. *Hydrological Processes, 22*(14), 2644–2656. https://doi.org/10.1002/hyp.6861.

Bae, S., & Chang, H. (2019). Urbanization and floods in the Seoul metropolitan area of South Korea: What old maps tell us. *International Journal of Disaster Risk Reduction, 37*, 101186. https://doi.org/10.1016/j.ijdrr.2019.101186.

Bini, L. M., Diniz-Filho, J. A. F., Rangel, T. F. L. V. B., Akre, T. S. B., Albaladejo, R. G., Albuquerque, F. S., ... Hawkins, B. A. (2009). Coefficient shifts in geographical ecology: An empirical evaluation of spatial and non-spatial regression. *Ecography, 32*(2), 193–204. https://doi.org/10.1111/j.1600-0587.2009.05717.x.

Bivand, R. (2017). Moran eigenvectors. Retrieved from https://cran.dcc.fc.up.pt/web/packages/spdep/vignettes/SpatialFiltering.pdf.

Brogna, D., Michez, A., Jacobs, S., Dufrêne, M., Vincke, C., & Dendoncker, N. (2017). Linking forest cover to water quality: A multivariate analysis of large monitoring datasets. *Water, 9*(3), 176. https://doi.org/10.3390/w9030176.

Chang, H. (2008). Spatial analysis of water quality trends in the Han River basin, South Korea. *Water Research, 42*(13), 3285–3304. https://doi.org/10.1016/j.watres.2008.04.006.

Chang, H., Park, K., & Bae, S.-H. (2019). Dreams and migration in South Korea's border region: Landscape change and environmental impacts. *Annals of the American Association of Geographers, 109*, 476–491. https://doi.org/10.1080/24694452.2018.1549471.

Chen, J., & Lu, J. (2014). Effects of land use, topography and socio-economic factors on river water quality in a mountainous watershed with intensive agricultural production in East China. *PLoS One, 9*(8), e102714. https://doi.org/10.1371/journal.pone.0102714.

Chun, Y. (2014). Analyzing Space–Time Crime Incidents Using Eigenvector Spatial Filtering: An Application to Vehicle Burglary. *Geographical Analysis, 46*(2), 165–184. https://doi.org/10.1111/gean.12034.

Chun, Y., Griffith, D. A., Lee, M., & Sinha, P. (2016). Eigenvector selection with stepwise regression techniques to construct eigenvector spatial filters. *Journal of Geographical Systems, 18*(1), 67–85. https://doi.org/10.1007/s10109-015-0225-3.

EGIS Korea (2017). Korea land cover. Retrieved September 5, 2017, from http://egis.me.go.kr/map/map.do?type=land.

Galloway, J. N., Aber, J. D., Erisman, J. W., Seitzinger, S. P., Howarth, R. W., Cowling, E. B., & Cosby, B. J. (2003). The nitrogen cascade. *AIBS Bulletin, 53*(4), 341–356.

Getis, A., & Griffith, D. A. (2002). Comparative spatial filtering in regression analysis. *Geographical Analysis, 34*(2), 130–140. https://doi.org/10.1111/j.1538-4632.2002.tb01080.x.

Grabowski, Z. J., Watson, E., & Chang, H. (2016). Using spatially explicit indicators to investigate watershed characteristics and stream temperature relationships. *Science of the Total Environment, 551–552*, 376–386. https://doi.org/10.1016/j.scitotenv.2016.02.042.

Griffith, D. A. (2010). Spatial filtering. *Handbook of applied spatial analysis* (pp. 301–318). . https://doi.org/10.1007/978-3-642-03647-7_16.

Hong, C.-Y., Chang, H., & Chung, E.-S. (2019). Comparing the functional recognition of aesthetics, hydrology, and quality in urban stream restoration through the framework of environmental perception. *River Research and Applications, 35*(6), 543–552. https://doi.org/10.1002/rra.3423.

Hoyer, W., & Chang, H. (2014). Assessment of freshwater ecosystem services in the Tualatin and Yamhill basins under climate change and urbanization. *Applied Geography, 53*, 402–416. https://doi.org/10.1016/j.apgeog.2014.06.023.

Isaak, D. J., Peterson, E. E., Ver Hoef, J. M., Wenger, S. J., Falke, J. A., Torgersen, C. E., ... Ruesch, A. S. (2014). Applications of spatial statistical network models to stream data. *Wiley Interdisciplinary Reviews Water, 1*(3), 277–294. https://doi.org/10.1002/wat2.1023.

Jacob, B. G., Muturi, E. J., Caamano, E. X., Gunter, J. T., Mpanga, E., Ayine, R., Okelloonen, J., Nyeko, J., Shililu, J. I., Githure, J. I., Regens, J. L., Novak, R. J., & Kakoma, I. (2008). Hydrological modeling of geophysical parameters of arboviral and protozoan disease vectors in Internally Displaced People camps in Gulu, Uganda. *International Journal of Health Geographics, 7*(1), 11. https://doi.org/10.1186/1476-072X-7-11.

Kim, D., Hirmas, D. R., McEwan, R. W., Mueller, T. G., Park, S. J., Šamonil, P., ... Wendroth, O. (2016). Predicting the influence of multi-scale spatial autocorrelation on soil–landform modeling. *Soil Science Society of America Journal, 80*(2), 409. https://doi.org/10.2136/sssaj2015.10.0370.

Kim, D., & Shin, Y. H. (2016). Spatial autocorrelation potentially indicates the degree of changes in the predictive power of environmental factors for plant diversity. *Ecological Indicators, 60*, 1130–1141. https://doi.org/10.1016/j.ecolind.2015.09.021.

King, R. S., Baker, M. E., Whigham, D. F., Weller, D. E., Jordan, T. E., Kazyak, P. F., & Hurd, M. K. (2005). Spatial considerations for linking watershed land cover to ecological indicators in streams. *Ecological Applications, 15*(1), 137–153. https://doi.org/10.1890/04-0481.

Korea Ministry of Environment (2016). Measurement data for water quality. Retrieved November 24, 2019, from http://water.nier.go.kr/waterMeasurement/selectWater.do.

Kuglerová, L., Ågren, A., Jansson, R., & Laudon, H. (2014). Towards optimizing riparian buffer zones: Ecological and biogeochemical implications for forest management. *Forest Ecology and Management, 334*, 74–84. https://doi.org/10.1016/j.foreco.2014.08.033.

Liberoff, A. L., Flaherty, S., Hualde, P., García Asorey, M. I., Fogel, M. L., & Pascual, M. A. (2019). Assessing land use and land cover influence on surface water quality using a parametric weighted distance function. *Limnologica, 74*, 28–37. https://doi.org/10.1016/j.limno.2018.10.003.

Lintern, A., Webb, J. A., Ryu, D., Liu, S., Bende-Michl, U., Waters, D., ... Western, A. W. (2018a). Key factors influencing differences in stream water quality across space. *Wiley Interdisciplinary Reviews Water, 5*(1), 1–31. https://doi.org/10.1002/wat2.1260.

Lintern, A., Webb, J. A., Ryu, D., Liu, S., Waters, D., Leahy, P., ... Western, A. W. (2018b). What are the key catchment characteristics affecting spatial differences in riverine water quality? *Water Resources Research, 54*(10), 7252–7272. https://doi.org/10.1029/2017WR022172.

Liu, J., Zhang, X., Wu, B., Pan, G., Xu, J., & Wu, S. (2017). Spatial scale and seasonal dependence of land use impacts on riverine water quality in the Huai River basin, China. *Environmental Science and Pollution Research, 24*(26), 20995–21010. https://doi.org/10.1007/s11356-017-9733-7.

Mainali, J., & Chang, H. (2018). Landscape and anthropogenic factors affecting spatial patterns of water quality trends in a large river basin, South Korea. *Journal of Hydrology, 564*, 26–40. https://doi.org/10.1016/j.jhydrol.2018.06.074.

Mainali, J., Chang, H., & Chun, Y. (2019). A review of spatial statistical approaches to modeling water quality. *Progress in Physical Geography: Earth and Environment, 43*(6), 801–826. https://doi.org/10.1177/0309133319852003.

de Mello, K., Valente, R. A., Randhir, T. O., dos Santos, A. C. A., & Vettorazzi, C. A. (2018). Effects of land use and land cover on water quality of low-order streams in Southeastern Brazil: Watershed versus riparian zone. *Catena, 167*, 130–138. https://doi.org/10.1016/j.catena.2018.04.027.

Miralha, L., & Kim, D. (2018). Accounting for and predicting the influence of spatial autocorrelation in water quality modeling. *ISPRS International Journal of Geo-Information, 7*(2), 64. https://doi.org/10.3390/ijgi7020064.

Ockenden, M. C., Hollaway, M. J., Beven, K. J., Collins, A. L., Evans, R., Falloon, P. D., & Haygarth, P. M. (2017). Major agricultural changes required to mitigate phosphorus losses under climate change. *Nature Communications, 8*(1), https://doi.org/10.1038/s41467-017-00232-0 Article number 161.

Peterson, E. E., Sheldon, F., Darnell, R., Bunn, S. E., & Harch, B. D. (2011). A comparison of spatially explicit landscape representation methods and their relationship to stream condition. *Freshwater Biology, 56*(3), 590–610. https://doi.org/10.1111/j.1365-2427.2010.02507.x.

Powers, S. M., Bruulsema, T. W., Burt, T. P., Chan, N. I., Elser, J. J., Haygarth, P. M., ... Zhang, F. (2016). Long-term accumulation and transport of anthropogenic phosphorus in three river basins. *Nature Geoscience, 9*(5), 353–356. https://doi.org/10.1038/ngeo2693.

Pratt, B., & Chang, H. (2012). Effects of land cover, topography, and built structure on seasonal water quality at multiple spatial scales. *Journal of Hazardous Materials, 209/210*, 48–58. https://doi.org/10.1016/j.jhazmat.2011.12.068.

R Core Team (2019). The R Project for Statistical Computing. Retrieved November 10, 2019, from https://www.r-project.org/.

Röman, E., Ekholm, P., Tattari, S., Koskiaho, J., & Kotamäki, N. (2018). Catchment characteristics predicting nitrogen and phosphorus losses in Finland. *River Research and Applications, 34*(5), 397–405. https://doi.org/10.1002/rra.3264.

Thayn, J. B., & Simanis, J. M. (2013). Accounting for spatial autocorrelation in linear regression models using spatial filtering with eigenvectors. *Annals of the Association of American Geographers, 103*(1), 47–66. https://doi.org/10.1080/00045608.2012.685048.

Tiefelsdorf, M., & Griffith, D. A. (2007). Semiparametric filtering of spatial autocorrelation: The eigenvector approach. *Environment and Planning A, 39*(5), 1193–1221. https://doi.org/10.1068/a37378.

WAMIS (2018). Water Resource Information Management System: Water Quality Standard. Retrieved May 7, 2018, from http://www.wamis.go.kr/wke/wke_wqbase_lst.aspx.

Watson, E. C., & Chang, H. (2018). Relation between stream temperature and landscape characteristics using distance weighted metrics. *Water Resources Management, 32*, 1167–1192. https://doi.org/10.1007/s11269-017-1861-9.

Xu, J., Yin, W., Ai, L., Xin, X., & Shi, Z. (2016). Spatiotemporal patterns of non-point source nitrogen loss in an agricultural catchment. *Water Science and Engineering, 9*(2), 125–133. https://doi.org/10.1016/j.wse.2016.03.003.